Am J Cancer Res 2022;12(7):3390-3404
www.ajcr.us /ISSN:2156-6976/ajcr0140324

Original Article

LMNB1, a potential marker for early prostate cancer progression

Jian-Hua Hong[1,2*], Sung-Tzu Liang[1*], Alexander Sheng-Shin Wang[3], Chia-Ming Yeh[1], Hsiang-Po Huang[4], Chia-Dong Sun[5,6], Zong-Han Zhang[7], Shih-Yu Lu[1], Yen-Hsiang Chao[1], Chung-Hsin Chen[1], Yeong-Shiau Pu[1]

[1]Department of Urology, National Taiwan University Hospital, Taipei, Taiwan; [2]Institute of Biomedical Engineering, National Taiwan University, Taipei, Taiwan; [3]Development Center for Biotechnology, Taipei, Taiwan; [4]Graduate Institute of Medical Genomics and Proteomics, National Taiwan University College of Medicine, Taipei, Taiwan; [5]Department of Pathology, National Taiwan University Hospital, Taipei, Taiwan; [6]Department and Graduate Institute of Forensic Medicine, College of Medicine, National Taiwan University, Taipei, Taiwan; [7]Institute of Chemistry, Academia Sinica, Taipei, Taiwan. [*]Equal contributors and co-first authors.

Received November 4, 2021; Accepted June 20, 2022; Epub July 15, 2022; Published July 30, 2022

Abstract: Although prostate cancer (PC) is the most common cancer among men in the Western world, there are no good biomarkers that can reliably differentiate between potentially aggressive and indolent PC. This leads to overtreatment, even for patients who can be managed conservatively. Previous studies have suggested that nuclear lamin proteins-especially lamin B1 (LMNB1)-play important roles in PC progression. However, the results of these studies are inconsistent. Here, we transfected the *LMNB1* gene into the telomerase reverse transcriptase-immortalized benign prostatic epithelial cell line, EP156T to generate a LMNB1-overexpressing EP156T (LMN-EP156T) cell line with increased cellular proliferation. However, LMN-EP156T cells could neither form colonies in soft agar, nor establish subcutaneous growth or metastasis in the xenograft NOD/SCID mouse model. In addition, immunohistochemical staining of LMNB1 in PC specimens from 143 patients showed a statistically significant trend of stronger LMNB1 staining with higher Gleason scores. A univariate analysis of the clinicopathological parameters of 85 patients with PC who underwent radical prostatectomy revealed that pathological stage, resection margin, and extracapsular extension were significant predictors for biochemical recurrence (BCR). However, LMNB1 staining showed only a non-significant trend of association with BCR (high vs. low staining: hazard ratio (HR), 1.83; 95% confidence interval (CI), 0.98-3.41; $P = 0.059$). In multivariate analysis, only pathological stage was a significant independent predictor of BCR (pT3 vs. pT2: HR, 2.29; 95% CI, 1.18-4.43; $P = 0.014$). In summary, LMNB1 may play a role in the early steps of PC progression, and additional molecular alterations may be needed to confer full malignancy potential to initiated cells.

Keywords: Prostate cancer, LMNB1, EP156T, invasion, metastasis, cancer biomarker

Introduction

In 2020, prostate cancer (PC) afflicted over 1.4 million patients and caused nearly 370,000 deaths worldwide [1]. The huge gap between the incidence and mortality rates in developed countries [2] suggests that many patients with PC die of causes other than PC, and that PC shows heterogeneous behavior and a wide range of tumor aggressiveness. The current risk-stratified management strategy for PC includes measures such as active surveillance in select patients, and has demonstrated survival rates comparable to those of immediate radical treatments [3]. Although conventional prognostic markers-such as serum prostate-specific antigen (PSA) and Gleason score (GS) grading-help stratify the risk of progression, over- and under-treatment are inevitable due to the inaccurate prediction of disease progression. Unfortunately, the personalized management of patients with PC remains to be developed due to the lack of powerful biomarkers [4]. As such, there is an urgent need to identify more novel biomarkers for PC progression.

To date, there are no perfectly accurate molecular markers that can differentiate potentially lethal PC from indolent ones. Studies have investigated a few prostate-specific markers in

the serum or prostate tissue, including PSA, prostate acid phosphatase, and prostate-specific membrane antigen [5]; however, none of these provide clinically useful information on PC progression. There is a general lack of early progression markers that play a pivotal role in disease progression and help inform decision-making between active surveillance and active treatments. For example, the loss of PTEN (a tumor suppressor) has been found to be associated with biochemical recurrence (BCR) after local treatment [6, 7]. In addition, PC is frequently accompanied by the TMPRSS2: ERG fusion caused by chromosomal translocation [8]. Both the above are predictors of BCR [9]. The overexpression of MMP2 [10] or FOXA1 [11] is associated with late progression events, such as metastasis. Overall, the aforementioned markers are primarily associated with late-stage PC progression. There are no good markers for early progression, which appears to be an unmet need in PC management.

Through a literature survey, we discovered that members of the lamin protein family may be involved in early-stage PC progression [12]. Lamin B1 (or LMNB1), in combination with lamin A/C or lamin B2 (LMNB2), constitutes the nuclear lamina that is scattered throughout the inner nuclear membrane and interacts with chromatin, binds to transcription factors, regulates gene transcription and DNA replication, and helps maintain the integrity of the nucleus [13-17]. Several cancers-including colorectal [18], ovarian [19], hepatocellular [20], pancreatic [21], and prostatic [22] cancer-are associated with increased levels of LMNB1; in contrast, the levels of lamin A/C vary among different cancers [23, 24]. Lung adenocarcinoma cell lines have been shown to overexpress LMNB1, and the knockdown of LMNB1 in these cell lines reduces their growth rate and colony forming ability [25]. In addition, a study reported that the suppression of LMNB1 expression induced cell apoptosis in a lung cancer model and attenuated their invasion ability in both *in vitro* experiments and in mouse models [26]. Hepatocellular carcinoma (HCC) tissues exhibit increased levels of LMNB1; as such, LMNB1 has been reported as an early biomarker for HCC [27].

Lamin A/C upregulation is associated with advanced stages of PC [28, 29]. However, there are major uncertainties regarding the role of LMNB1 in PC progression. Saarinen et al. reported that LMNB1 expression was associated with clinicopathological variables in the whole cohort, but not in the cohort with high GS (GS ≥ 7). The same study also showed that LMNB1 was not associated with PC specific mortality in either the whole PC cohort or the high-GS cohort [12]. However, the researchers used only tissue microarrays to investigate the role of altered LMNB1 expression, and did not conduct mechanistic studies of LMNB1 function. In contrast, Luo et al. demonstrated that LMNB1 upregulation was associated with BCR, metastasis, and survival in PC [30].

To further elucidate the role of LMNB1 in PC progression, we used *in vitro* cell lines, animal models, and clinical approaches in the current study. We found that LMNB1 may very likely be involved in the early steps of PC progression. Based on our findings, we suggest that LMNB1 is a good potential biomarker for early PC progression.

Materials and methods

EP156T prostate epithelial cells and transfection with lentiviral vectors harboring LMNB1

A human *TERT*-immortalized EP156T prostatic epithelial cell line was purchased from the American Type Culture Collection (CRL3289™, ATCC, Manassas, VA, USA) and grown in MCDB-153 medium supplemented with bovine pituitary extract (25 mg/500 ml medium), hEGF (5 ng/ml medium), 1% fetal bovine serum (FBS), and 0.5 μg/ml puromycin. The cells were stored in a humid incubator supplied with 5% CO_2 at 37°C. The EP156T cells [31] were used as the *in vitro* model to investigate the role of LMNB1 overexpression in PC progression. LMNB1-overexpressing EP156T (LMN-EP156T) cells were obtained by transfecting EP156T cells with *LMNB1*-harboring lentiviral vectors (pLAS2w-neo derived) at a multiplicity of infection (moi) of 3, followed by G418 selection (80 μg/ml) over a 4-week period. The map of the pLAS2w-neo lentiviral vector is shown in **Figure 1**. Mock EP156T were cells transfected with lentiviruses produced from the pLAS2w-neo vector without *LMNB1*. The LNCaP, DU145, and PC-3 cell lines were provided by Dr. Hsiang-Po Huang at the Graduate Institute of Medical Genomics and Proteomics of National Taiwan University, College of Medicine. These

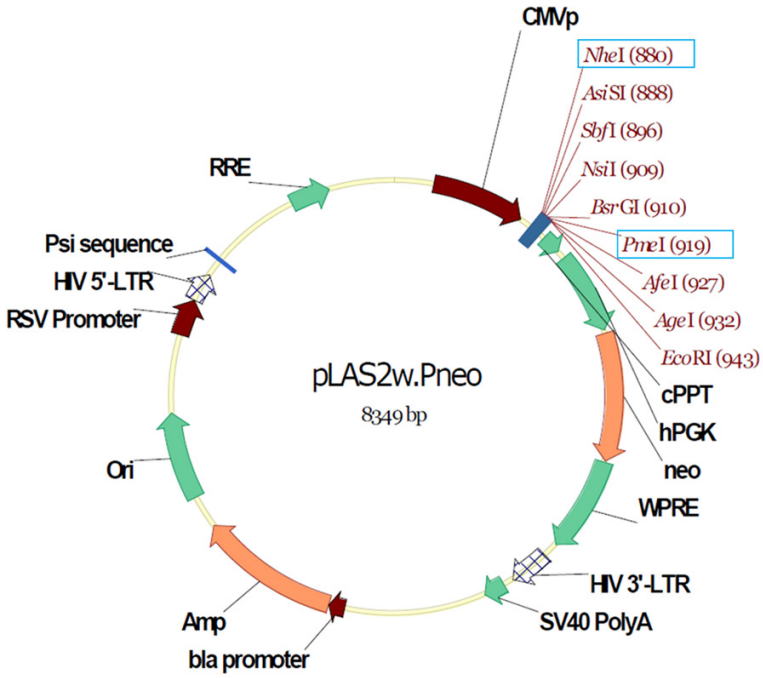

Figure 1. Map of the lentiviral vector pLAS2w.Pneo. The full length of human LMNB1 cDNA (1,761 bp) is cloned into multiple cloning sites between the *Nhe*I and *Pme*I restriction sites on the vector, driven by the CMV promoter. The downstream neomycin (neo)-resistant gene is driven by the human PGK promoter.

were used as positive controls of LMNB1 expression and/or the xenograft metastasis model in animal experiments.

Western blotting to confirm LMNB1 expression

A total of 30 μg of total protein was extracted from the EP156T, Mock EP156T, LMN-EP156T, LNCaP, DU145, and PC-3 cells. The proteins were resolved on 10% SDS-PAGE, transferred onto nitro-cellulous paper, probed with primary rabbit polyclonal antibodies against LMNA (#2032, Cell Signaling, Danvers, MA, USA), LMNB1 (TA349381, OriGene, Rockville, MD, USA), and GAPDH (TA890003, OriGene, Rockville, MD, USA), subsequently probed with horseradish peroxidase (HRP)-conjugated mouse anti-rabbit IgG antibody (Santa Cruz, sc-2357, Dallas, TX, USA), and then detected with enhanced chemiluminescence using the Amersham™ ECL™ Prime Western Blotting Detection reagent (RPN2232, GE Healthcare Life Sciences, Buckinghamshire, UK). The protein signal bands for LMNA, LMNB1, and GAPDH were visualized using an ImageQuant™ LAS 4000 biomolecular imager (GE Healthcare Life Sciences, Uppsala, Sweden) and quantified with the Image Quan 8.0L software.

Immunohistochemical staining for LMNB1 expression

Immunohistochemical (IHC) staining of LMNB1 expression was done to reveal the expression levels in cells. PC-3 cells were used as positive controls [32]. EP156T, Mock EP156T, LMN-EP156T, and PC-3 cells were grown on slides and fixed in 4% paraformaldehye in phosphate buffered saline (PBS) for 30 minutes. After rinse in PBS, cells were permeated in 0.1% Triton X-100 in PBS for 15 minutes, and antigen was retrieved at 100°C for 10 min in citrate buffer (0.24% [w/v] sodium citrate dihydrate, 0.04% [w/v] citric acid monohydrate; pH 6.0). Endogenous peroxidase activity was blocked using 0.3% hydrogen peroxide solution for 10 min at room temperature. After 5 min of PBS wash for three times, slides were incubated with blocking solution (3% BSA and 10% normal goat serum in PBS) for 90 minutes at room temperature to block non-specific binding. Cells were then incubated with a rabbit anti-LMNB1 polyclonal antibody (1:4000 dilution; TA349381, OriGene, Rockville, MD, USA) at 4°C overnight, followed by immunoassay using DAKO EnVision detection system (K5007, Agilent Technologies, Glostrup, Denmark). Cells were counterstained with Mayer hematoxylin, dehydrated with gradient alcohol, and fixed with mounting glue. Negative control staining was done using PBS to replace the primary antibody solution.

Measurement of the cell proliferation by MTS assay

To compare the cell proliferation rate between cell lines, we performed the MTS assay (G3580, Promega, Madison, WI, USA). A total of 6.5 × 10^3 cells in 0.1 ml of complete medium were seeded into each well of 96 well-plates in triplicate for each cell line. In addition,

5 plates were prepared for measurement at each of 5 time points (4, 21, 28, 45, and 52 h) after seeding. One plate at each time point was used for the MTS assay. A 20 μl aliquot of MTS reagent was added to each well and the plates were incubated for 1 h at 37°C in an incubator supplied with 5% CO_2. The absorbance at 490 nm was measured using an ELISA reader (BioTek, Winooski, VT, USA). For this assay, we did not include G418 in the culture medium. The absorbance readings at 490 nm were plotted as a function of growth time and represented as the mean ± SEM (standard error of the means).

Measurement of cell invasiveness by a Matrigel-coated transwell assay

A total of 5×10^4 cells of each cell line in 0.1 ml medium + 0.1% FBS were seeded onto the inserts of a 24-well plate (pore size, 8 μM) (REF No. 3422, Costar, Lowell, MA, USA) precoated with Matrigel. The insert wells were placed on receiver wells with 0.65 ml of medium + 10% FBS per well. The 24-well plate was incubated in a humid incubator supplied with 5% CO_2 at 37°C for 48 h. Following this, the cells were stained with 0.25% crystal violet in 20% methanol for 10 min. Before staining, the cells on the apical side of the insert wells were removed with swabs, such that only those cells that had passed the membrane could be visualized after staining.

Colony forming assay

A total of 5×10^3 cells of each cell line were mixed in 0.3% melt soft agar containing complete growth medium and plated onto a culture dish (3.5 cm in diameter). The plates were incubated at 37°C in a humid incubator supplied with 5% CO_2 for 2 weeks before the pictures were taken.

Immunohistochemical staining of LMNB1 expression in surgical specimens of the prostate

Formalin-fixed paraffin-embedded archival PC tissues from 85 radical prostatectomies (RP) and 58 transurethral resections of the prostate (TURP) were used for the immunohistochemical (IHC) staining of nuclear LMNB1 expression. Relevant clinical data including patient demographics, tumor characteristics, and biochemical recurrence were recorded. The study was approved by the Research Ethical Committee of the hospital (approval no. 201712093RINB). There were 30, 30, 30, 23, and 30 PC tumor blocks that were graded as GS 3+3, 3+4, 4+3, 4+4, and ≥ 4+5, respectively. Tissue sections were deparaffinized, followed by antigen retrieval using the Epitope Retrieval 1 solution (pH 6.0, Leica Biosystems, Wetzlar, Germany) at 100°C for 20 min. The slides were stained in the BOND-MAX autostainer (Leica Biosystems) using the Bond detection kit according to the manufacturer's protocols. Briefly, the tissue sections were blocked in the blocking solution for 5 min and then sequentially probed with primary antibodies against LMNB1 (1:300; TA349381, OriGene) for 30 min and with a Polymer-HRP reagent for 8 min. Staining was developed for 5 min with DAB as the substrate chromogen. The sections were then counterstained with modified Mayer's hematoxylin for 7 min. All the reactions were carried out at room temperature (25°C). The slides were washed three times with the Bond wash solution between steps. Stained tissue sections were photographed under a Nikon Eclipse Ts2 inverted microscope (Nikon, Tokyo, Japan).

Xenograft mouse model

The animal experiment was approved by the Institutional Animal Care and Use Committee (IACUC, approval no. 20201017) and followed the IACUC guidelines. The experiment was conducted to test whether LMNB1 overexpression allowed the EP156T cells to grow and/or metastasize in the xenograft mouse model. A total of 2×10^6 cells of the PC-3 (positive control), EP156T, Mock EP156T, and LMN-EP156T cell lines were subcutaneously injected into one side of the lateral chest walls of 8-week-old male NOD/SCID mice provided by BioLASCO Taiwan Co., Ltd. A total of 5 mice were injected with each cell line. The tumor size and body weight of the mice were monitored twice a week. Once the tumor had reached a size of 1.5 cm in diameter, the mice were sacrificed. The subcutaneous tumors, lymph nodes, livers, lungs, brains, and the prostate were dissected, fixed in 10% neutrally buffered formalin, embedded in paraffin, and sectioned at 5 μm for hematoxylin and eosin staining.

Association between LMNB1 expression and BCR in the TCGA patient cohort

Between 2000 and 2013, a total of 497 patients who received RP for PC were enrolled in the TCGA database. After excluding 3 patients

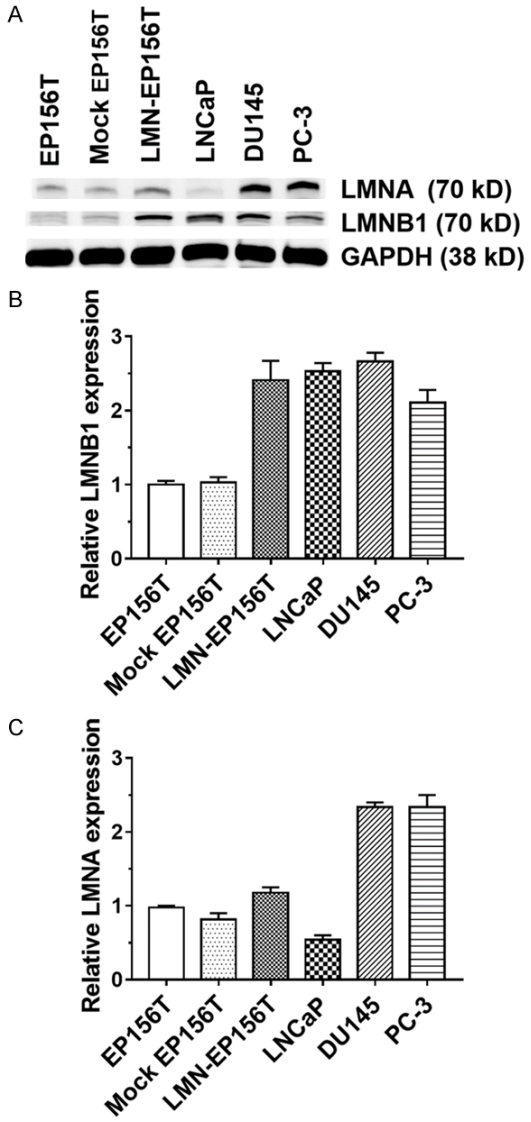

Figure 2. Western blotting to detect the expression levels of LMNA and LMNB1 in cells. (A) The protein signal bands for LMNA, LMNB1, and GAPDH. (B, C) The relative expression levels of LMNB1 and LMNA (normalized to GAPDH expression) in different cell lines. The mean ± SEM of two independent experiments are shown ($P = 0.0005$ and $P < 0.0001$ for LMNB1 and LMNA, respectively; ANOVA). The results show that LMNB1-overexpressing EP156T (LMN-EP156T) cells express significantly higher amounts of LMNB1 than the parental and Mock EP156T cells. All three prostate cancer cell lines express high levels of LMNB1. All cells express LMNA, with PC-3 and DU145 expressing higher amounts of LMNA than the other cells.

with missing LMNB1 expression levels and 5 patients with unknown disease-recurrence status, we included a total of 489 patients in our analysis. Univariable Cox regression analysis was used to evaluate the association between various parameters and disease-free survival (DFS). Multivariable analysis was used to identify the independent predictors for DFS. We divided patients with PC into high-expression and low-expression groups based on the median LMNB1 expression (310 ± 11.2).

Statistical analysis

The clinicopathological parameters were compared between groups of patients in our clinical cohort using Fisher's exact test (for categorical variables) and the Mann-Whitney U test (for continuous variables with non-normal distribution). The Kruskal-Wallis test was used to analyze the differences in LMNB1 IHC scores between patient groups categorized by GS values (143 PC patients; 85 RP and 58 TURP). Trend analysis was applied with the analysis of variance (ANOVA) to reveal the association between GS and LMNB1 IHC scores.

The clinical outcome of interest was BCR after RP, defined as the time point when the PSA level in the serum was ≥ 0.2 ng/ml. BCR-free survival was defined as the period between the date of RP and the date when the serum PSA was ≥ 0.2 ng/ml. Univariable and multivariable Cox proportional-hazards regression analysis and the log-rank test were used to evaluate the prognostic implications of various clinicopathologic parameters (including the LMNB1 IHC score) for BCR.

All statistical calculations were two-tailed and considered statistically significant at $P < 0.05$. Statistical analyses were performed using the IBM SPSS statistical software (version 26; IBM Corp., Armonk, NY, USA) and GraphPad Prism (version 8; GraphPad Software, San Diego, CA, USA).

Results

LMNB1-overexpressing EP156T cells

The Western blotting results are shown in **Figure 2A**. The expression ratio of LMNB1 to GAPDH was higher in LMN-EP156T cells than in the parental cells or Mock EP156T cells. There were no differences in LMNB1 expression levels between the parental and Mock EP156T cells. The LMN-EP156T cells expressed high levels of LMNB1 similar to those expressed by the 3 cell lines used as positive

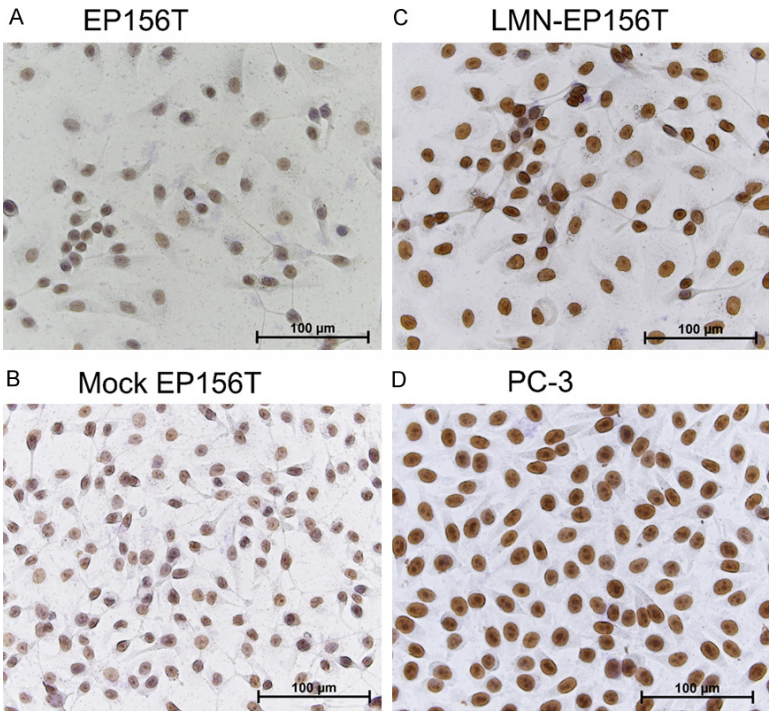

Figure 3. Immunohistochemical (IHC) staining of LMNB1 expression. Staining results were shown for (A) parental EP156T, (B) Mock EP156T, (C) LMNB1-overexpressing EP156T (LMN-EP156T), and (D) PC-3 cells (positive control). Both LMN-EP156T and PC-3 cells expressed strong nuclear staining of LMNB1, which was higher than either parental EP156T or Mock EP156T cells.

controls (LNCaP, DU145, and PC-3). This confirmed that the LMN-EP156T cells over-expressed LMNB1 (**Figure 2B**). LMNA expression levels were high in the DU145 and PC-3 cells and low in all other cells, including the LMN-EP156T cells (**Figure 2C**). The expressions of LMNB1 in parental, Mock, LMN-EP156T, and PC-3 cells (positive control) were also determined and compared by IHC staining. The results of IHC staining for LMNB1 were consistent with those of Western blotting (**Figure 3**).

Higher cell proliferation rate in LMNB1-overexpressing EP156T cells

All the three cell lines reached a growth plateau at 48 h. However, the LMN-EP156T cells grew faster than the parental and Mock EP156T cells (**Figure 4**; $P < 0.01$ by ANOVA).

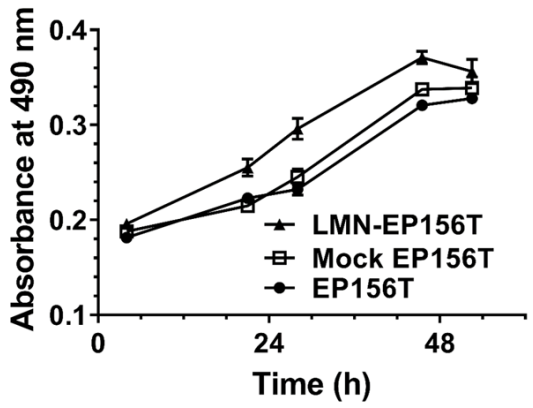

Figure 4. MTS assay to measure the rate of cell growth. A total of 6.5 × 10^3 cells in 0.1 ml of complete medium were seeded onto each well of 96 well-plates in triplicate for each cell line. Five repeated plates were prepared for measurements at 5 time points. At each time point, one plate was used for this assay. MTS reagent (20 μl) was added to each well, and the plates were incubated at 37°C for 1 h. The absorbance at 490 nm is shown as the mean ± SEM of three independent experiments. LMNB1-overexpressing EP156T (LMN-EP156T) cells show significantly faster growth compared to the other two cell lines ($P < 0.01$; ANOVA).

LMNB1 overexpression enhanced the invasion ability of cells

The Matrigel-coated transwell assay demonstrated that compared to the parental and Mock EP156T cells, LMN-EP156T cells could digest the Matrigel and pass through the 8-μm pores at a faster rate, and formed larger colonies beneath the transwell after 48 h (**Figure 5**).

Colony-forming assay

The results of colony-forming assays showed that the parental EP156T (**Figure 6A**), Mock EP156T (**Figure 6B**), and LMN-EP156T (**Figure 6C**) cells did not form visible colonies on soft agar after 2 weeks of incubation at 37°C. In contrast, the PC-3 cells (positive control) formed numerous colonies (**Figure 6D**). These results suggested that LMNB1 overexpression may not be sufficient for cells to evade contact inhibition, and may not induce tumorigenesis in immortalized EP156T cells.

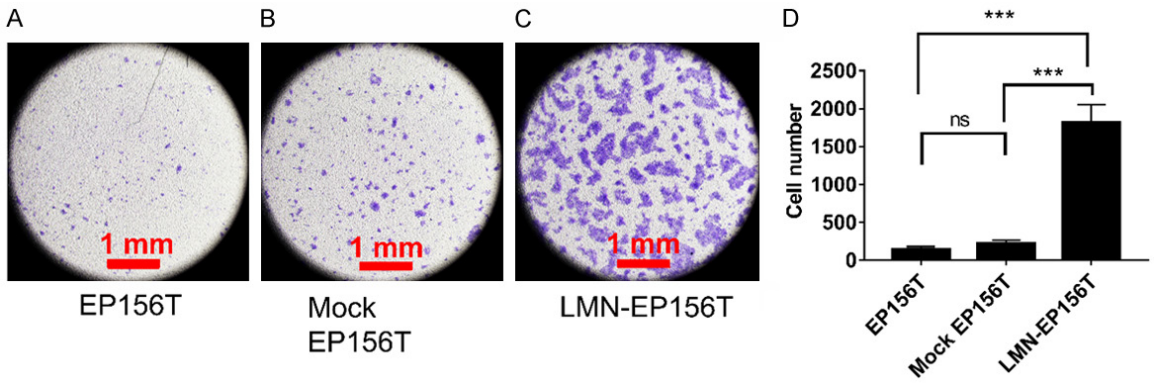

Figure 5. Matrigel-coated transwell assay (37 °C for 48 h, 40 × magnification). A total of 5 × 10^4 cells of each cell line in 0.1 ml medium + 0.1% FBS were seeded onto an insert well (pore size, 8 μm) for a 24-well plate pre-coated with Matrigel. The insert wells were placed on receiver wells with 0.65 ml of medium + 10% FBS per well. After incubation at 37 °C for 48 h, the cells on the apical side of the insert wells were removed with swabs. Only cells that had passed the membrane could be visualized after staining in 20% methanol with 0.25% crystal violet for 10 min. The results are shown for (A) EP156T, (B) Mock EP156T, and (C) LMN-EP156T cells. (D) The number of cells that penetrated the wells are shown as the mean ± SEM of three independent experiments. Statistical significance was determined by ANOVA ($P < 0.0001$). Significantly more LMNB1-overexpressing EP156T (LMN-EP156T) cells passed through the 8-μm pores than parental and Mock EP156T cells.

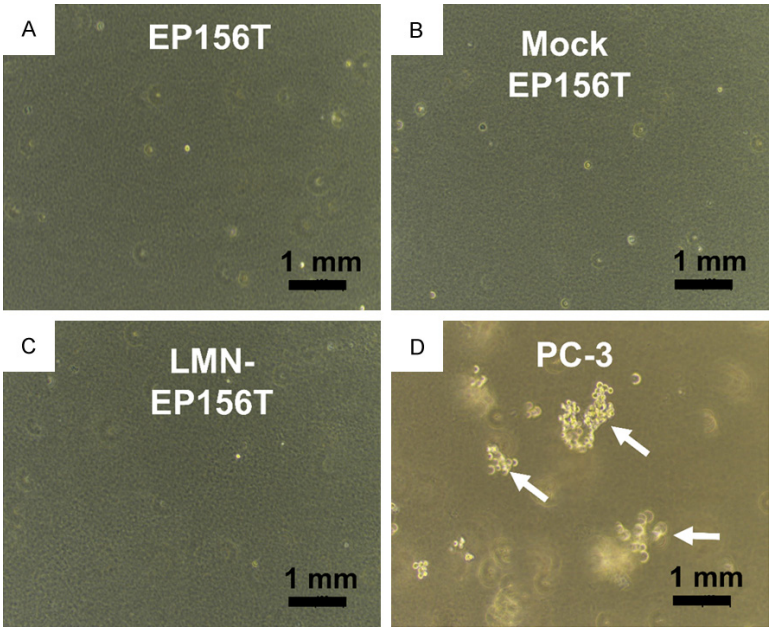

Figure 6. Colony-formation assay. Results are shown for (A) EP156T, (B) Mock EP156T, (C) LMNB1-overexpressing EP156T (LMN-EP156T), and (D) PC-3 cells. A total of 5 × 10^3 cells of each cell line were mixed in 0.3% soft agar with complete growth medium, and plated onto a culture dish (diameter, 3.5 cm). Numerous colonies can be seen in the plates inoculated with PC-3 after 2 weeks of incubation (magnification, 100 ×) at 37 °C. However, no colonies have formed in the plates inoculated with the other cell lines. White arrows indicate PC-3 cell colonies.

LMNB1 expression levels in PC surgical specimens, as measured by IHC staining

Figure 7 shows the LMNB1 expression levels in PC specimens with graded GS. The staining results clearly showed that the higher the GS, the higher the LMNB1 staining scores (**Figure 7F**; $P < 0.0001$ by ANOVA). Both the GS 4+4 and GS ≥ 4+5 tumors had the highest median IHC scores. LMNB1 staining was significantly higher in GS 4+3 tumors than in GS 3+4 tumors ($P = 0.010$, Mann-Whitney U test). However, there were no significant differences between the GS 3+3 and 3+4 tumors or between the GS 4+4 and ≥ 4+5 tumors ($P = 0.344$ and $P = 1.00$, respectively, Mann-Whitney U test), indicating that LMNB1 may play a pivotal role in early PC progression.

Xenograft mouse model

The PC-3 cells (positive control) formed subcutaneous tumors in 4 of the 5 xenografted mice (**Figure 8**). The tumors were palpable at 2 weeks after injection. The average body weight of the PC-3-xenografted mice was 26.9 ± 2.6 g (mean ± SEM), and the average tumor volume was 3232 ± 627 mm^3 at the time of sacrifice (end of the 7^{th} week after injection). However,

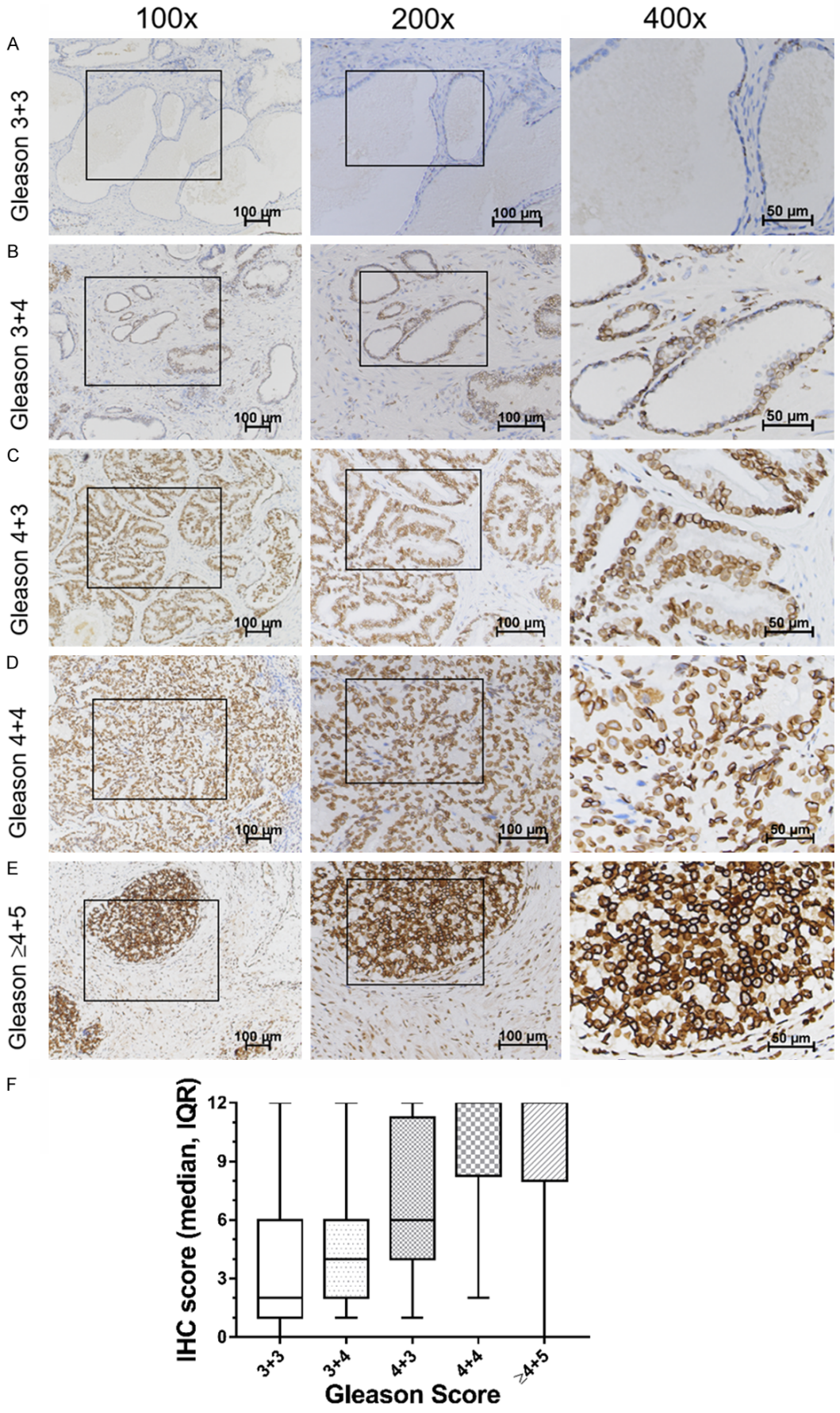
100x
200x
400x
A
Gleason 3+3
B
Gleason 3+4
C
Gleason 4+3
D
Gleason 4+4
E
Gleason ≥4+5
100 μm
50 μm
F
IHC score (median, IQR)
0
3
6
9
12
3+3
3+4
4+3
4+4
≥4+5
Gleason Score

Figure 7. Immunohistochemical (IHC) staining of LMNB1 cells in archival paraffin blocks of prostate cancer tissues with graded Gleason scores (GS). (A-E) Representative block sections graded as GS 3+3, 3+4, 4+3, 4+4, and ≥ 4+5, respectively. Each row shows the same block section at different magnifications, as indicated at the top of each column. (F) LMNB1 IHC scores in tumors (N = 143) classified according to GS. The IHC staining of 143 archival paraffin blocks was evaluated by a qualified pathologist (Dr. Sun, CD) using a scoring system based on the percentage (0: no staining; 1: 1%-25%; 2: 26%-50%; 3: 51%-75%; 4: 76%-100%) and intensity (0: negative; 1: weak; 2: moderate; 3: intense) of IHC staining. An immune-reactivity score (range, 0-12) was obtained by multiplying the percentage and intensity scores. There is a significant trend, showing that the higher the GS, the higher the LMNB1 IHC score (trend analysis by ANOVA; $P < 0.0001$). The box plots show the median and interquartile range, and the whiskers indicate the minimum and maximum scores in each GS category. The medians of the GS 4+4 and GS ≥ 4+5 groups reach 100%.

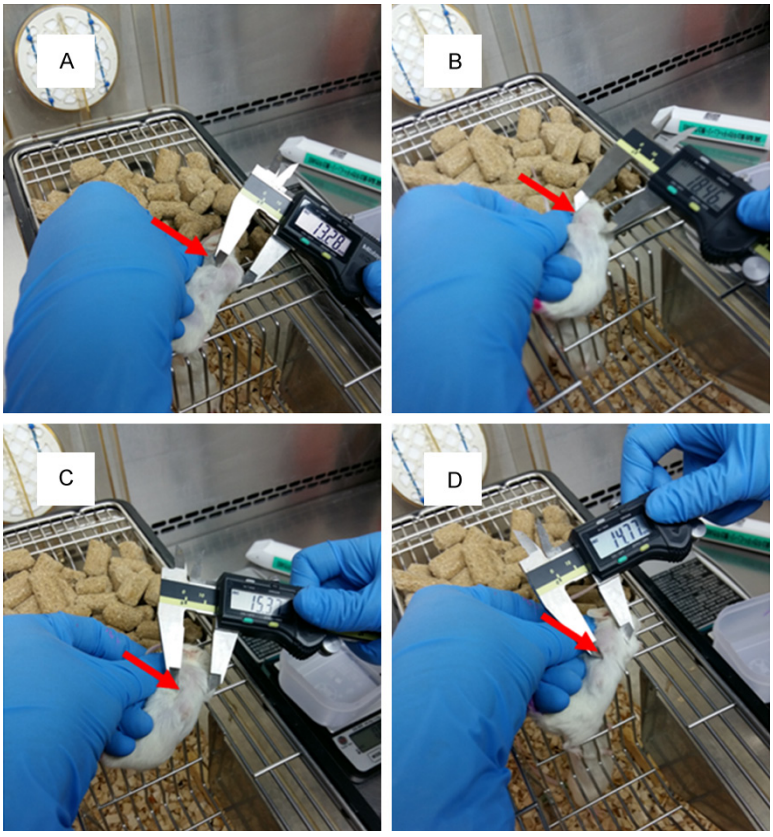

Figure 8. Xenograft mouse model showing evident subcutaneous tumors in the right chest 7 weeks after the injection of PC-3 cells. (A-D) Four of the five mice injected with PC-3 cells formed subcutaneous tumors (red arrows). The tumor sizes range between 13 mm and 19 mm in diameter. No tumors were seen in mice injected with EP156T, Mock EP156T, or LMNB1-overexpressing EP156T cells (photos not shown).

there were no visible subcutaneous tumors in mice injected with EP156T, Mock EP156T or LMN-EP156T cells at the end of the 14th week after injection. Among all mice organs harvested for examination, only the lymph nodes (4 of 5 mice) and lungs (4 of 5 mice) were found to have metastatic lesions in the PC-3-xenografted mice (**Figure 9A**, **9B**). There were no metastatic lesions found in any organs from mice injected with EP156T, Mock EP156T, or LMN-EP156T cells.

Association between LMNB1 expression and BCR in our cohort

The clinicopathological characteristics of the 143 PC patients are listed in **Table 1**. Compared to patients who received RP, those who received palliative TURP were significantly older and had higher PSA levels, clinical stage, and GS values at diagnosis. However, there was no significant difference in the LMNB1 IHC score between the RP and TURP groups. Univariable Cox regression analysis showed that pT3, positive resection margin, and extracapsular extension were associated with a significantly higher risk of BCR (**Table 2**). LMNB1 IHC scores showed a non-significant association with BCR (hazard ratio (HR), 1.83; 95% confidence interval (CI), 0.98-3.41; $P = 0.059$). In the multivariate analysis, only pathological stage significantly predicted BCR (pT3 vs. pT2: HR, 2.29; 95% CI, 1.18-4.43; $P = 0.014$; **Table 2**) after adjustment for resection margin and LMNB1 IHC score.

Association of LMNB1 expression with disease recurrence in the TCGA cohort

The median LMNB1 expression in the TCGA cohort was 310 ± 11.2. After excluding patients with missing LMNB1 expression levels or disease recurrence status, disease recurrence occurred in 45 (27%) of 165 patients with high

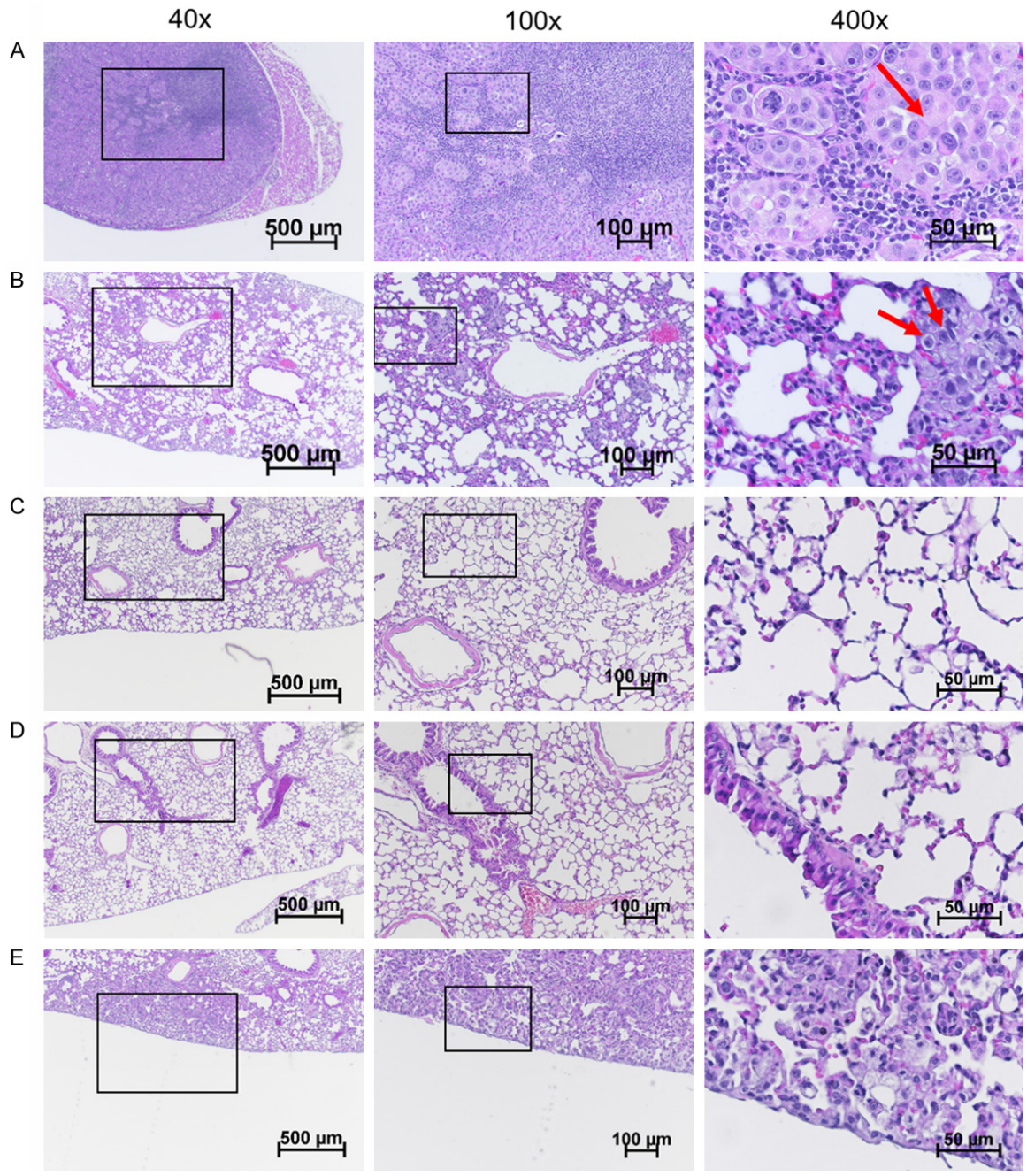

Figure 9. Hematoxylin and eosin-stained tissue sections from xenografted mice. (A) An enlarged and metastasized lymph node from the PC-3-injected mouse. (B-E) Lung sections from mice injected with PC-3, EP156T, Mock EP156T, and LMNB1-overexpressing EP156T cells, respectively. Each row shows the same section with increasing magnification. Red arrows indicate PC-3 metastatic cell nests with clear nucleoli in either the lymph node (A) or lung (B). There are no subcutaneous growths or metastatic lesions in mice injected with the parental, Mock, or LMNB1-overexpressing EP156T cells.

LMNB1 levels, but in only 46 (14%) of 324 patients with low LMNB1 levels. The median DFS of patients with high LMNB1 expression was 69.1 months (95% CI, 60.1-79.1), which was significantly lower than that of patients with low LMNB1 expression (below the median). The univariable Cox-regression analysis indicated that high LMNB1 expression was related to a higher risk of disease recurrence (high vs. low expression: HR, 2.32; 95% CI,

Table 1. Clinicopathological characteristics of patients with prostate cancer

	RP (N = 85)	PALLIATIVE TURP (N = 58)	*P*-VALUE
AGE			
MEDIAN, IQR	70.0 (67.0-74.0)	81.0 (74.8-87.3)	< 0.001
< 75	57 (67%)	24 (41%)	0.002
≥ 75	28 (33%)	34 (59%)	
	Patient no. (%)	Patient no. (%)	
PROSTATE-SPECIFIC ANTIGEN AT DIAGNOSIS*			0.002
< 10	39 (48%)	18 (31%)	
10-20	25 (31%)	11 (19%)	
≥ 20	17 (21%)	29 (50%)	
CLINICAL T STAGE			< 0.001
CT1	38 (46%)	17 (29%)	
CT2	36 (43%)	5 (9%)	
CT3/CT4†	9 (11%)	36 (62%)	
GLEASON SCORE			< 0.001
3+3	11 (13%)	19 (33%)	
3+4	30 (35%)	0 (0%)	
4+3	26 (31%)	4 (7%)	
≥ 4+4	18 (21%)	35 (60%)	
LMNB1 IHC SCORE			0.391
LOW	51 (60%)	30 (52%)	
HIGH	34 (40%)	28 (48%)	

Abbreviations: RP, radical prostatectomy; TURP, transurethral resection of the prostate; IQR, interquartile range; IHC, immunohistochemical staining. LMNB1 IHC scores were categorized into two groups: grades 1-7 (low) and grades 8-12 (high). *Four patients in the RP group had missing data for prostate-specific antigen at diagnosis. †Two patients in the RP group had missing data for clinical T stage.

1.54-3.51; $P < 0.001$; **Table 3**). However, after adjustment for other parameters, LMNB1 expression was a non-significant predictor of DFS (HR, 1.47; 95% CI, 0.95-2.28; $P = 0.086$; **Table 3**). Only pathological stage was independently associated with poor DFS (pT3/4 vs. pT2: HR, 1.97; 95% CI, 1.05-3.70; $P = 0.034$).

Discussion

In the current study, we demonstrated that LMNB1 overexpression allowed faster cell proliferation and enhanced transwell invasion in the immortalized human prostatic epithelial cell line. However, LMNB1 overexpression did not induce colony formation in soft agar or subcutaneous growth or metastasis in the xenograft mouse model. We also showed that IHC staining for LMMB1 expression correlated well with the GS of clinical tumor specimens. The higher the LMNB1 IHC staining, the higher the tumor GS. In the LMNB1 IHC staining of clinical tumors, GS 4+3 tumors showed significantly higher staining than GS 3+4 tumors. In contrast, there was only a marginally insignificant difference between GS 3+3 and 3+4 tumors, and no significant difference between GS 4+4 and GS ≥ 4+5 tumors. These results suggested that LMNB1 was involved in the progression of tumors from GS 3 to GS 4, but not from GS 4 to GS 5. All the above findings suggested that LMNB1 may be an early (rather than late) biomarker of PC progression.

Kogan et al. [31] characterized EP156T cells in 2006, showing that these cells retained most characteristics of prostate epithelial basal cells (such as p63-positivity). In addition, EP156T cells could differentiate into early and late prostate buds, but failed to terminally differentiate when cultured in 2% Matrigel. Although EP156T cells can undergo epithelial-mesenchymal transition accompanied by loss of contact inhibition, they cannot form colonies in soft agar [33]. In this study, we showed that even *LMNB1*-transfected EP156T cells (LMN-EP156T cells) could not form colonies, indicating that LMNB1 overexpression alone is not adequate to confer tumor cell stemness [34] or transform EP156T into a fully malignant cell line.

Table 2. Univariable and multivariable Cox-regression analyses of biochemical recurrence in the radical prostatectomy group

VARIABLES	UNIVARIABLE			MULTIVARIABLE		
	HR	95% CI	*P*-value	HR	95% CI	*P*-value
AGE						
< 75	Referent					
≥ 75	0.58	0.29-1.16	0.124			
PROSTATE-SPECIFIC ANTIGEN AT DIAGNOSIS						
≤ 10	Referent					
10-20	1.46	0.72-2.93	0.292			
≥ 20	1.62	0.70-3.75	0.258			
GLEASON SCORE						
3+3	Referent	-				
3+4	1.09	0.34-3.46	0.891			
≥ 4+3	2.21	0.77-6.36	0.14			
PATHOLOGICAL STAGE						
pT2	Referent			Referent		
pT3	2.86	1.51-5.41	0.001	2.29	1.18-4.43	0.014
RESECTION MARGIN						
NEGATIVE	Referent			Referent		
POSITIVE	2.34	1.03-5.29	0.041	2.05	0.89-4.73	0.093
EXTRACAPSULAR EXTENSION						
ABSENCE	Referent					
PRESENCE	2.35	1.26-4.41	0.007			
LYMPHOVASCULAR INVASION						
ABSENCE	Referent					
PRESENCE	1.12	0.56-2.24	0.751			
LMNB1 IHC SCORE						
LOW	Referent			Referent		
HIGH	1.83	0.98-3.41	0.059	1.63	0.86-3.10	0.137

Variables were selected for multivariate analysis based on their prognostic significance in the univariate analysis ($P < 0.05$). Significant single variables were chosen for univariate analysis after the exclusion of potential high-association variables in different models. The LMNB1 IHC score was categorized into two groups: grades 1-7 (low) and grades 8-12 (high). Abbreviations: CI, confidence interval; HR, hazard ratio.

We established an *in vitro* cell model of PC progression by transfecting a specific candidate gene into *TERT* gene-immortalized EP156T cells. We believe that this cell line model may provide insights into early events during PC progression. The transfected EP156T cell line model is different from established cancer cell lines (such as LNCaP, DU145, or PC-3) in which the genetic changes necessary for malignant transformation are readily available. It may be difficult and inappropriate to investigate early disease progression events using these advanced cancer cell lines. This is because it may be impossible to observe the early progression phenotype in these sophisticated cancer cell lines without disabling multiple genes simultaneously. As shown in **Figure 2**, the three above-mentioned cancer cell lines expressed abundant LMNB1. It may be interesting to examine the consequences of disabling the function of LMNB1 in these cancer cell lines.

LMNB1 is also known as LMN, ADLD, LMN2, LMNB, and MCPH26 (https://www.ncbi.nlm.nih.gov/gene/4001). Although a few published studies have investigated the role of LMNB1 in PC progression, their results were inconsistent. In our cohort, the IHC staining of LMNB1 in 143 PC tumors showed a significant trend of increasing LMNB1 expression with higher GS. However, LMNB1 expression was only marginally associated with BCR ($P = 0.059$) in patients

Table 3. Univariable and multivariable Cox-regression analyses of disease-free survival in the TCGA cohort

	Patients (N)	Events (N)	UNIVARIABLE			MULTIVARIABLE		
			HR	95% CI	*P*-value	HR	95% CI	*P*-value
AGE								
< 61	199	32	Referent					
≥ 61	290	59	1.46	0.95-2.25	0.084			
GLEASON SCORE								
3+3	45	1	Referent	-				
3+4	145	12	3.70	0.48-28.45	0.209	3.41	0.44-26.56	0.241
≥ 4+3	299	78	12.59	1.75-90.49	0.012	7.43	1.00-55.23	0.050
PATHOLOGICAL STAGE								
pT2	185	14	Referent					
pT3/T4	298	74	3.70	2.09-6.56	< 0.001	1.97	1.05-3.70	0.034
UNKNOWN	6	0	-	-	-	-	-	-
PATHOLOGICAL LYMPH NODE								
ABSENT	321	56	Referent					
PRESENT	78	23	1.86	1.14-3.03	0.013	1.06	0.64-1.77	0.811
UNKNOWN	90	12	0.78	0.42-1.46	0.443	0.96	0.51-1.83	0.910
POSITIVE MARGIN								
ABSENT	312	46	Referent					
PRESENT	148	43	2.27	1.50-3.45	< 0.001	1.65	1.06-2.58	0.028
UNKNOWN	29	2	0.50	0.12-2.08	0.344	0.36	0.09-1.50	0.161
LMNB1 EXPRESSION LEVEL								
LOW	324	46	Referent					
HIGH	165	45	2.32	1.54-3.51	< 0.001	1.47	0.95-2.28	0.086

LMNB1 expression was categorized into two groups: > 310 (high) and < 310 (low). Abbreviations: CI, confidence interval; HR, hazard ratio.

with RP (N = 85). Using the rank aggregation method and gene co-expression network analysis, Song, et al. found that LMNB1 was among four differentially expressed genes (DEGs) that could be used for the diagnosis and prognosis of PC. Specifically, higher LMNB1 expression levels were associated with higher GS [35], which is consistent with our findings. Using the databases of two PC cohorts (TCGA and LSK-CC), Luo et al. showed that high LMNB1 expression was associated with PC metastasis and poor patient survival [30]. This is inconsistent with our results, as we did not observe a significant association between LMNB1 expression and BCR. Indeed, our analysis using the TCGA dataset revealed a statistically non-significant association between LMNB1 expression levels and DFS ($P = 0.086$) after the exclusion of ineligible patients. Saarinen et al. [12] reported that GS, PSA, pathological stage, and the LMNB1 IHC score were significantly associated with BCR in both univariable and multivariable Cox regression analyses of the entire cohort. However, in the high-risk cohort (GS ≥ 7), only GS and PSA-but not the LMNB1 IHC score-significantly predicted BCR in the multivariate analysis, suggesting that LMNB1 may be an early marker for disease progression in PC. The same study also showed that LMNB1 expression was not significantly associated with PC-specific survival in the entire cohort or in the high-risk cohort (GS ≥ 7).

Although our study supports the involvement of LMNB1 in early stages of PC progression, other clinicopathological parameters-such as pathological stage, GS, margin status, or certain genetic makers-may play more important roles than LMNB1 at clinically relevant endpoints. Multiple hits along the course of PC progression (apart from LMNB1 upregulation) may be necessary to push cancer cells to metastasize and become lethal.

Acknowledgments

The study was sponsored by a national research grant, MOST-107-2314-B-002-032-MY3. We thank Miss Liu, Yu-Ju (a veterinarian) and Miss Tsai, Yi-Ting (a veterinarian pathologist) for their help in the animal experiments. We also thank Miss Tzu-Fan Wu (a research assistant) for her assistance in experimental work.

Disclosure of conflict of interest

None.

Address correspondence to: Drs. Chung-Hsin Chen and Yeong-Shiau Pu, Department of Urology, National Taiwan University Hospital, Taipei, Taiwan. E-mail: mufasachen@gmail.com (CHC); yspu@ntu.edu.tw (YSP)

References

[1] Sung H, Ferlay J, Siegel RL, Laversanne M, Soerjomataram I, Jemal A and Bray F. Global cancer statistics 2020: GLOBOCAN estimates of incidence and mortality worldwide for 36 cancers in 185 countries. CA Cancer J Clin 2021; 71: 209-249.

[2] Hassanipour-Azgomi S, Mohammadian-Hafshejani A, Ghoncheh M, Towhidi F, Jamehshorani S and Salehiniya H. Incidence and mortality of prostate cancer and their relationship with the Human Development Index worldwide. Prostate Int 2016; 4: 118-124.

[3] Lane JA, Donovan JL, Davis M, Walsh E, Dedman D, Down L, Turner EL, Mason MD, Metcalfe C, Peters TJ, Martin RM, Neal DE and Hamdy FC; ProtecT study group. Active monitoring, radical prostatectomy, or radiotherapy for localised prostate cancer: study design and diagnostic and baseline results of the ProtecT randomised phase 3 trial. Lancet Oncol 2014; 15: 1109-1118.

[4] Loeb S, Bjurlin MA, Nicholson J, Tammela TL, Penson DF, Carter HB, Carroll P and Etzioni R. Overdiagnosis and overtreatment of prostate cancer. Eur Urol 2014; 65: 1046-1055.

[5] Pentyala S, Whyard T, Pentyala S, Muller J, Pfail J, Parmar S, Helguero CG and Khan S. Prostate cancer markers: an update. Biomed Rep 2016; 4: 263-268.

[6] Chaux A, Peskoe SB, Gonzalez-Roibon N, Schultz L, Albadine R, Hicks J, De Marzo AM, Platz EA and Netto GJ. Loss of PTEN expression is associated with increased risk of recurrence after prostatectomy for clinically localized prostate cancer. Mod Pathol 2012; 25: 1543-1549.

[7] Lotan TL, Wei W, Morais CL, Hawley ST, Fazli L, Hurtado-Coll A, Troyer D, McKenney JK, Simko J, Carroll PR, Gleave M, Lance R, Lin DW, Nelson PS, Thompson IM, True LD, Feng Z and Brooks JD. PTEN loss as determined by clinical-grade immunohistochemistry assay is associated with worse recurrence-free survival in prostate cancer. Eur Urol Focus 2016; 2: 180-188.

[8] Tomlins SA, Rhodes DR, Perner S, Dhanasekaran SM, Mehra R, Sun XW, Varambally S, Cao X, Tchinda J, Kuefer R, Lee C, Montie JE, Shah RB, Pienta KJ, Rubin MA and Chinnaiyan AM. Recurrent fusion of TMPRSS2 and ETS transcription factor genes in prostate cancer. Science 2005; 310: 644-648.

[9] Yoshimoto M, Joshua AM, Cunha IW, Coudry RA, Fonseca FP, Ludkovski O, Zielenska M, Soares FA and Squire JA. Absence of TMPRSS2: ERG fusions and PTEN losses in prostate cancer is associated with a favorable outcome. Mod Pathol 2008; 21: 1451-1460.

[10] Gohji K, Fujimoto N, Hara I, Fujii A, Gotoh A, Okada H, Arakawa S, Kitazawa S, Miyake H, Kamidono S and Nakajima M. Serum matrix metalloproteinase-2 and its density in men with prostate cancer as a new predictor of disease extension. Int J Cancer 1998; 79: 96-101.

[11] Gerhardt J, Montani M, Wild P, Beer M, Huber F, Hermanns T, Müntener M and Kristiansen G. FOXA1 promotes tumor progression in prostate cancer and represents a novel hallmark of castration-resistant prostate cancer. Am J Pathol 2012; 180: 848-861.

[12] Saarinen I, Mirtti T, Seikkula H, Boström PJ and Taimen P. Differential predictive roles of A- and B-type nuclear lamins in prostate cancer progression. PLoS One 2015; 10: e0140671.

[13] Guelen L, Pagie L, Brasset E, Meuleman W, Faza MB, Talhout W, Eussen BH, de Klein A, Wessels L and de Laat W. Domain organization of human chromosomes revealed by mapping of nuclear lamina interactions. Nature 2008; 453: 948-951.

[14] Kumaran RI and Spector DL. A genetic locus targeted to the nuclear periphery in living cells maintains its transcriptional competence. J Cell Biol 2008; 180: 51-65.

[15] Shimi T, Pfleghaar K, Kojima S, Pack CG, Solovei I, Goldman AE, Adam SA, Shumaker DK, Kinjo M, Cremer T and Goldman RD. The A- and B-type nuclear lamin networks: microdomains involved in chromatin organization and transcription. Genes Dev 2008; 22: 3409-3421.

[16] Shumaker DK, Solimando L, Sengupta K, Shimi T, Adam SA, Grunwald A, Strelkov SV, Aebi U, Cardoso MC and Goldman RD. The highly con-

served nuclear lamin Ig-fold binds to PCNA: its role in DNA replication. J Cell Biol 2008; 181: 269-280.
[17] Camps J, Erdos MR and Ried T. The role of lamin B1 for the maintenance of nuclear structure and function. Nucleus 2015; 6: 8-14.
[18] Alfonso P, Canamero M, Fernández-Carbonié F, Núñez A and Casal JI. Proteome analysis of membrane fractions in colorectal carcinomas by using 2D-DIGE saturation labeling. J Proteome Res 2008; 7: 4247-4255.
[19] Bengtsson S, Krogh M, Szigyarto CA, Uhlen M, Schedvins K, Silfverswärd C, Linder S, Auer G, Alaiya A and James P. Large-scale proteomics analysis of human ovarian cancer for biomarkers. J Proteome Res 2007; 6: 1440-1450.
[20] Lim SO, Park SJ, Kim W, Park SG, Kim HJ, Kim YI, Sohn TS, Noh JH and Jung G. Proteome analysis of hepatocellular carcinoma. Biochem Biophys Res Commun 2002; 291: 1031-1037.
[21] Li L, Du Y, Kong X, Li Z, Jia Z, Cui J, Gao J, Wang G and Xie K. Lamin B1 is a novel therapeutic target of betulinic acid in pancreatic cancer. Clin Cancer Res 2013; 19: 4651-4661.
[22] Coradeghini R, Barboro P, Rubagotti A, Boccardo F, Parodi S, Carmignani G, D'Arrigo C, Patrone E and Balbi C. Differential expression of nuclear lamins in normal and cancerous prostate tissues. Oncol Rep 2006; 15: 609-613.
[23] Irianto J, Pfeifer CR, Ivanovska IL, Swift J and Discher DE. Nuclear lamins in cancer. Cell Mol Bioeng 2016; 9: 258-267.
[24] Denais C and Lammerding J. Nuclear mechanics in cancer. Adv Exp Med Biol 2014; 773: 435-470.
[25] Li W, Li X, Li X, Li M, Yang P, Wang X, Li L and Yang B. Lamin B1 overexpresses in lung adenocarcinoma and promotes proliferation in lung cancer cells via AKT pathway. Onco Targets Ther 2020; 13: 3129-3139.
[26] Tang D, Luo H, Xie A, He Z, Zou B, Xu F, Zhang W and Xu X. Silencing LMNB1 contributes to the suppression of lung adenocarcinoma development. Cancer Manag Res 2021; 13: 2633-2642.
[27] Sun S, Xu MZ, Poon RT, Day PJ and Luk JM. Circulating Lamin B1 (LMNB1) biomarker detects early stages of liver cancer in patients. J Proteome Res 2010; 9: 70-78.
[28] Skvortsov S, Schäfer G, Stasyk T, Fuchsberger C, Bonn GK, Bartsch G, Klocker H and Huber LA. Proteomics profiling of microdissected low- and high-grade prostate tumors identifies Lamin A as a discriminatory biomarker. J Proteome Res 2011; 10: 259-268.
[29] Kong L, Schäfer G, Bu H, Zhang Y, Zhang Y and Klocker H. Lamin A/C protein is overexpressed in tissue-invading prostate cancer and promotes prostate cancer cell growth, migration and invasion through the PI3K/AKT/PTEN pathway. Carcinogenesis 2012; 33: 751-759.
[30] Luo F, Han J, Chen Y, Yang K, Zhang Z and Li J. Lamin B1 promotes tumor progression and metastasis in primary prostate cancer patients. Future Oncol 2021; 17: 663-673.
[31] Kogan I, Goldfinger N, Milyavsky M, Cohen M, Shats I, Dobler G, Klocker H, Wasylyk B, Voller M and Aalders T. hTERT-immortalized prostate epithelial and stromal-derived cells: an authentic in vitro model for differentiation and carcinogenesis. Cancer Res 2006; 66: 3531-3540.
[32] Yang A, Zhao Y, Wang Y, Zha X, Zhao Y, Tu P and Hu Z. Huaier suppresses proliferative and metastatic potential of prostate cancer PC3 cells via downregulation of Lamin B1 and induction of autophagy. Oncol Rep 2018; 39: 3055-3063.
[33] Ke XS, Qu Y, Goldfinger N, Rostad K, Hovland R, Akslen LA, Rotter V, Øyan AM and Kalland KH. Epithelial to mesenchymal transition of a primary prostate cell line with switches of cell adhesion modules but without malignant transformation. PLoS One 2008; 3: e3368.
[34] Thomson SP and Meyskens FL Jr. Method for measurement of self-renewal capacity of clonogenic cells from biopsies of metastatic human malignant melanoma. Cancer Res 1982; 42: 4606-4613.
[35] Song ZY, Chao F, Zhuo Z, Ma Z, Li W and Chen G. Identification of hub genes in prostate cancer using robust rank aggregation and weighted gene co-expression network analysis. Aging (Albany NY) 2019; 11: 4736-4756.